Optimization of Neutron Chopper and Optics for CENTAUR, the SANS/WANS Diffractometer at the Spallation Neutron Source Second Target Station

Shuo Qian*, Cristina Boone, Feng Ye, Yuanpeng Zhang

Oak Ridge National Laboratory

*Corresponding author:

Shuo Qian qians@ornl.gov

Notice: This manuscript has been authored by UT-Battelle, LLC, under contract DE-AC05-00OR22725 with the US Department of Energy (DOE). The US government retains and the publisher, by accepting the article for publication, acknowledges that the US government retains a nonexclusive, paid-up, irrevocable, worldwide license to publish or reproduce the published form of this manuscript, or allow others to do so, for US government purposes. DOE will provide public access to these results of federally sponsored research in accordance with the DOE Public Access Plan (http://energy.gov/downloads/doe-public-access-plan).

Abstract

This report presents the physics design and optimization of the neutron chopper and optics systems for the CENTAUR instrument, a multifunctional small-angle and wide-angle neutron scattering diffractometer for the Spallation Neutron Source Second Target Station. This instrument will offer a wide range of capabilities, including small-angle neutron scattering with wide Q coverage (e.g., 0.001–20 $Å^{-1}$), providing a tool to investigate structures from atomic to mesoscopic scales simultaneously. To efficiently transport desired neutrons from the compact high-brightness cold source, several innovative designs are utilized: a time-zero chopper with a straight guide system for short-wavelength neutrons, octagonal guides for higher flux, and a correlation chopper to reduce inelastic scattering. The optimization process considers factors such as usable time-integrated flux, instrument resolution, brilliance transfer, divergence, and acceptance diagram uniformity. The overall design prioritizes flexibility to accommodate diverse user requirements.

Keywords

Neutron scattering, optics, correlation chopper, SANS, WANS, diffractometer

Introduction

Neutron scattering is a powerful technique that enables researchers to investigate the structure and dynamics of materials with significant penetration depth. Its advantages include sensitivity to light elements, a broad range of length and time scales, and the ability to perform nondestructive measurements. In line with the Second Target Station (STS) project of the Spallation Neutron Source (SNS) at Oak Ridge National Laboratory (ORNL), the CENTAUR instrument has been selected for one of the initial suites of instruments to be designed and constructed [1]. CENTAUR is multifunctional, serving as a workhorse and high-performance small-angle neutron scattering (SANS) instrument with wide-angle and diffraction capabilities. It enables wide Q coverage up to the diffraction region, allowing investigations spanning from atomic to mesoscopic scales simultaneously, with measurement time for structural evolution/change as good as a few seconds for certain systems.

CENTAUR's performance relies heavily on the high-brightness cold neutron beam from STS. Neutrons at STS will be generated by short pulses of protons with an energy of 1.3 GeV and a total beam power of 700 kW that bombard a water-cooled, rotating, solid tungsten target. These pulses are directed from the upgraded SNS accelerator [2]. The spallation neutrons are subsequently moderated into cold neutrons by two low-dimensional para-hydrogen moderators surrounded by a light-water premoderator and a beryllium reflector. To achieve optimal performance, the design incorporates a short distance between the high-density spallation target and the compact moderator–reflector assembly, pure para-hydrogen as the neutron moderator, and small moderator-viewed areas (3 × 3 cm for higher energy resolution in the upper cylinder moderator and 3 cm in diameter for higher time-averaged flux in the lower tube moderator) [3]. This configuration allows for the extraction of high-brightness cold neutrons. CENTAUR, specifically, is positioned to directly view one of the outlets of the lower tube moderator to take advantage of the higher time-averaged cold neutron flux.

This work focuses on the optimization of neutron delivery, encompassing the chopper system and the optics system of CENTAUR. These components are crucial for neutron-scattering beamlines because

they facilitate the removal of unwanted neutrons and the precise definition and transportation of required neutrons to the sample, directly influencing divergence, flux, beam profile, and the scattering data. Within the CENTAUR user community, a consensus regarding the instrument's requirements has been established: CENTAUR will be a high-performance SANS instrument with wide Q coverage, capable of covering from 0.001 to 20 $Å^{-1}$ in a single measurement. The typical sample sizes will be 10 mm in diameter with smaller beams possible. With this broad Q coverage, the priority is to design the instrument to ensure a highly collimated beam to achieve the low Q required by SANS. The instrument can adjust beam divergence for different SANS experiments. A secondary goal is to expand the Q range to wide-angle and diffraction regions by additional detector coverage and the broad wavelength band from the source. This expanded Q range, while secondary, is an important capability gap to be filled at SNS. It will provide simultaneous measurement on hierarchical structure evolution from atomic to mesoscopic scales. This report presents optimization results along with several innovative designs. Notable introductions include octagonal guides to enhance neutron transport and a correlation chopper to minimize inelastic neutron scattering. All these features should allow CENTAUR to offer a state-of-the-art tool for the community to study fast kinetic, in-situ or in-vivo structural changes in many hierarchical systems. The design and concept presented could not only interest future users but also serve as a valuable reference for developing similar instruments in the future.

Before presenting our results, we first comment on our general approach for the figure-of-merit during the optimization. Selecting a single figure-of-merit poses a challenge for this type of instrument because the community is very diverse and has different requirements regarding characteristics such as instrument Q resolution, and minimum Q (Q_{min}). The instrument's Q resolution requirement varies greatly depending on sample characteristics, including polydispersity, crystallinity, and disorder, particularly for small-angle scattering. Therefore, CENTAUR is designed to be adjustable by collimation flexibility (a control for both divergence and flux), which is achieved by using a variable optics system with interchangeable apertures and neutron guides. The collimation from the SANS configuration is always

good for diffraction, but to achieve the large Q range required, the wavelength band is adjustable from 0.5 to 2 Å by using a pair of bandwidth-defining choppers. For a given configuration, the most critical factor is the time-integrated flux (neutrons per second per square centimeter ($n\ s^{-1}\ cm^{-2}$)) at the sample position because it significantly influences the successful completion of an experiment within the constraints of beam time and sample quantity. Therefore, brilliance transfer serves as a measure of effective neutron transport for the optics between the source and the sample position [4]. Q_{min} is important, and this high-performance SANS instrument will achieve 0.001 $Å^{-1}$. The parameters were decoupled if the consequences of change were clear. However, if consequences were less clear (e.g., the guide m-value), then the staring location and size were grouped to run a multiparameter optimization. The current engineering reality imposed some constraints. Thus, the outcomes are evaluated based on direct consequences of certain parameter changes, balancing factors such as integrated flux, flux for specific wavelength bands, brilliance transfer, divergence, and phase space uniformity [5,6].

Background considerations, including instrument and sample backgrounds, are vital. However, this study did not involve investigating the instrument background because its simulation is beyond the capability of the McStas code. Sample background, inherent to sample yet different from one to another, is also a challenge for meaningful simulations.

Methods and Materials

McSTAS

The Monte Carlo simulation for the choppers and optics were performed with McStas package with the latest STS source file. Typically, simulations used at least 10^9 neutrons for each run to ensure acceptable statistics. McStas simulations were performed by varying the targeted parameters while holding the known or already optimized parameters as constants.

Correlation chopper experiment at CORELLI

Polycrystalline Si from NIST (SRM640) was used as the test sample. They were mixed with different H_2O/D_2O ratios (100%, 50%, and 0% D_2O) and sealed in the aluminum powder sample can (5 mm diameter) provided by SNS. The experiment was performed in the CORELLI instrument, which was equipped with a correlation chopper. The SNS source ran at 60 Hz, and the correlation chopper at CORELLI ran at 294 Hz asynchronously with the source pulse to provide a full spectrum of incident energies. This process enables an equal average transmission probability for the whole wavelength band for the correlation analysis. [7] The data were reduced using Mantid software with the correlation analysis off and on for comparison.

Guide misalignment simulation

The misalignment deviations were categorized and defined as follows: (1) transversal: a displacement perpendicular to the beam direction, either vertical (y) or horizontal (x); (2) longitudinal: a displacement along the beam (z); (3) orientational: a rotation around the beam z-axis. The whole CENTAUAR guide system was divided into eight sections according to their locations, and each section comprised of 0.5 m guide elements, which were typical from guide vendors. The misalignment on a section level and an element level is additive. The deviations imposed on section and on element were randomized using normal distributions with different expected values as inputs. A wide range of deviations were simulated: section transversal 50 – 200 μm, section rotational 2 – 8 mrad, element transversal 20–100 μm, element rotational 0.4–2 mrad. The simulation was parallelly executed in 100 nodes, with each node 1×10^{10} neutrons for a set of section parameters.

Results and Discussions

1. Overall instrument length and layout

The overall instrument length and layout were optimized for known physical constraints. As shown in Fig. 1(A), the instrument will start with fixed neutron guides inside the source's monolith structure. The shutters and various choppers are inside the bunker, which has a radius of 14.36 m. The fixed guides

bridge gaps between choppers and shutters to maximize neutron transport. A variable optics system outside the bunker wall employs interchangeable neutron guides or source-defining apertures to provide different collimation lengths. This mechanism is the primary way to adjust the divergence and flux on the sample, and it must be located outside the bunker to enable routine maintenance. A section of V-cavity guide can be inserted at the starting section of the variable optics system to provide neutron polarization [8].

As a SANS instrument, the collimation length and the longest available wavelength are important to achieve the necessary small angle for Q_{min}, as determined by Eq. (1):

$$Q = \frac{4\pi \sin\theta}{\lambda} \#(1)$$

where θ is half of the scattering angle, λ is the neutron wavelength.

To reach the required $Q_{\min}$ of 0.001 Å^{-1} with the maximum wavelength 15 Å, a symmetric layout was used. The maximum collimation distance ($L_1^{\max}$) and the maximum sample-to-detector distance ($L_2^{\max}$) were both set to 10 m. Then, the total length of the instrument L_{md}, the distance from the moderator face to the farthest detector surface, can be established. The value of L_{md} also determined the neutron bandwidth and the source repetition rate f:

$$\Delta\lambda = \lambda_{\max} - \lambda_{\min} = \frac{h}{m}\frac{1}{L_{\mathrm{md}} f} \#(2)$$

In principle, for a source repetition rate of 15 Hz or of 7.5 Hz with every other pulse skipped (the frame-skip mode), a shorter L_{md} can be used to provide a wide-wavelength bandwidth. This configuration may translate to a broad dynamic Q coverage, but it reduces available collimation length to reach the required $Q_{\min}$. A longer L_1 can be used for improved collimation, but the resultant reduced wavelength bandwidth reduces the integrated flux. These factors along with the engineering constraint of the bunker wall outer radius and other necessary components such as the removeable polarization V-cavity outside the bunker wall, the balanced choice is L_{md} = 35.5 m.

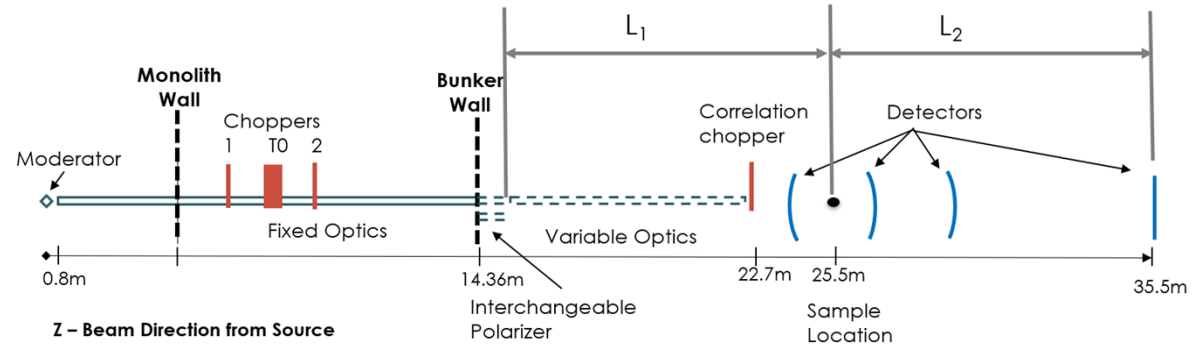

(A)

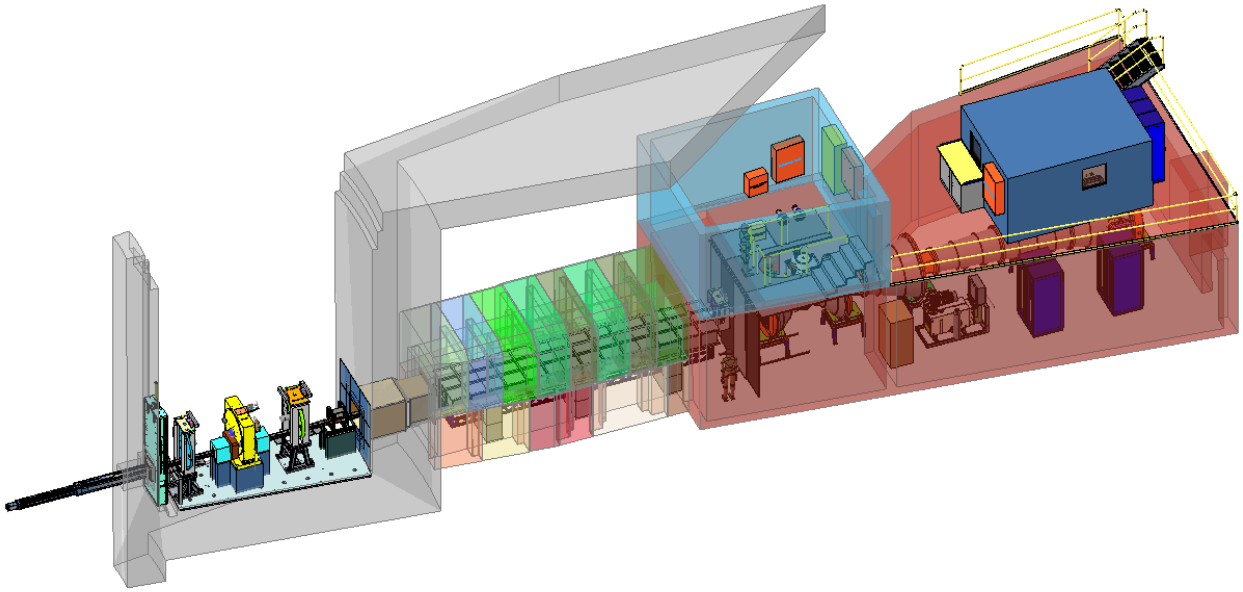

(B)

Figure 1. (A) Layout and dimensions of the instrument. The major components are as labeled. The L_1 (collimation distance) shown is the maximum L_1^{max} = 10 m, the L_2 (sample-to-detector distance) shown is L_2^{max} = 10 m. The detectors include a backscattering detector array and three forwarding detector arrays. (B) An isotropic view of the current design of CENTAUR

Therefore, the theoretical wavelength band at 15 Hz is $\Delta\lambda$ = 7.44 Å and covers from, e.g., 2–9.44 Å or 0.5–7.94 Å, providing the dynamic factor ($Q_{max}/Q_{min} = \lambda_{max}/\lambda_{min}$) of 4.77 or 15.88, respectively. For 7.5 Hz, the bandwidth doubles to $\Delta\lambda$ = 14.88 Å, e.g., for a wavelength range of 2–16.88 Å or 0.5–15.38 Å with the dynamic factor of 8.44 or 30, respectively. The latter dynamic factor is imperative for the

instrument to cover the widest Q range required in a single configuration, 0.001–20 $Å^{-1}$). The neutron emission time uncertainty will reduce the usable fraction of bandwidth from the full frame band by about ~20%, which again emphases the importance of the total length. Increasing the total length by a few meters is undesirable because it will significantly reduce the dynamic factor. The optimized length of 35.5 m balances the needs of long collimation and a wide wavelength band.

2. Chopper system

2.1 Bandwidth-defining chopper

The bandwidth chopper is used to define the wavelength bandwidth Δλ. Placing the chopper closer to the source reduces the possible leakage from other pulses. For STS, the bunker outside the target monolith provides an excellent space for housing choppers (Fig. 1(B)). Chopper locations are constrained by the outer radius of the target monolith (~6 m) and the inner radius of the bunker (11.64 m). Placing choppers inside the bunker allows easier access for installation and maintenance. To provide maximum usable bandwidth and flexibility, the optimized choice is a two-chopper system: one single-disc chopper (Chopper 1) and one double-disc chopper (Chopper 2) (Fig. 1). The bandwidth then can be defined at one chopper's leading open edge and the other chopper's trailing edge. Thus, the precision requirement for the opening cut angle can be relaxed. The additional flexibility is provided by the double-disc chopper. By reconfiguring the relative phase of the two discs, more flexible control of the bandwidth can be achieved. Chopper 1's opening is 80°, and Chopper 2's opening is 120°, and their locations are set at 6.25 and 9.68 m, respectively. The transmission diagrams show that no leakage occurs up to 70 Å for both 15 and 7.5 Hz (Supplemental information [SI] Fig. S1). A frame-overlap mirror is not necessary; it would produce an unfavorable nonuniform beam profile. Additionally, the chopper relative phase can be adjusted further to restrict the wavelength band as needed for calibration and other special purposes.

2.2 The choice of a T0 chopper vs. bender guide

When the proton beam is injected into the neutron-producing target, high-energy fast neutrons that are undesirable for a neutron-scattering experiment must be blocked to reduce the instrumental background. Two options are available: (1) a time-zero (T0) chopper for a straight beamline, with a rotor of a thick Inconel blade to block fast neutrons in synchronization with the source frequency, and (2) a curved beamline to shield the downstream from the source's direct line of sight.

For the first option, the STS standard large T0 chopper with rotor diameter 1.24 m will be located 8 m from the source, between the bandwidth-defining choppers inside the bunker. The beam is 3 cm in diameter, so the chopper is fully open for neutron wavelengths larger than 0.268 Å.

The second option involves bender optics with 12 sections of 3-channel guides. Each is 0.5 m long and angled 0.092° to each other. Together, the assembly blocks the source away from the direct line of sight at the sample position, but thermal and cold neutrons can still be transported. The guide's dimensions (3 × 3 cm) match the tube moderator size. An m = 5 supermirror coating was used for all surfaces in the simulation. The choice represented an achievable, yet costly, solution for bender optics that can be compared with the T0 chopper option.

Compared with a straight guide, the shorter wavelength neutrons (e.g., <2 Å) were severely lost by the bender optics (Fig. 2) in the simulation. The much-reduced flux for wavelengths shorter than2 Å can be further seen in Fig. 2A and 2B. The acceptance diagrams calculated for 0.5 Å and 1 Å neutrons at the location 8 m from the source (the end of the bender optics) and at the sample position (Fig. S2 in SI) also indicate the significant loss. In particular, the much needed 0.5–1 Å neutrons are reduced to almost none at the sample position. Although the longer wavelength neutrons do not suffer such unbearable loss, the bender induces additional nonuniformity in the beam divergence. This nonuniformity can be clearly seen in the separated acceptance diagram from the horizontal direction, in which the bender curve acceptance (Fig.2C) is much worse than a straight guide with a gap for T0 chopper (Fig. 2D).

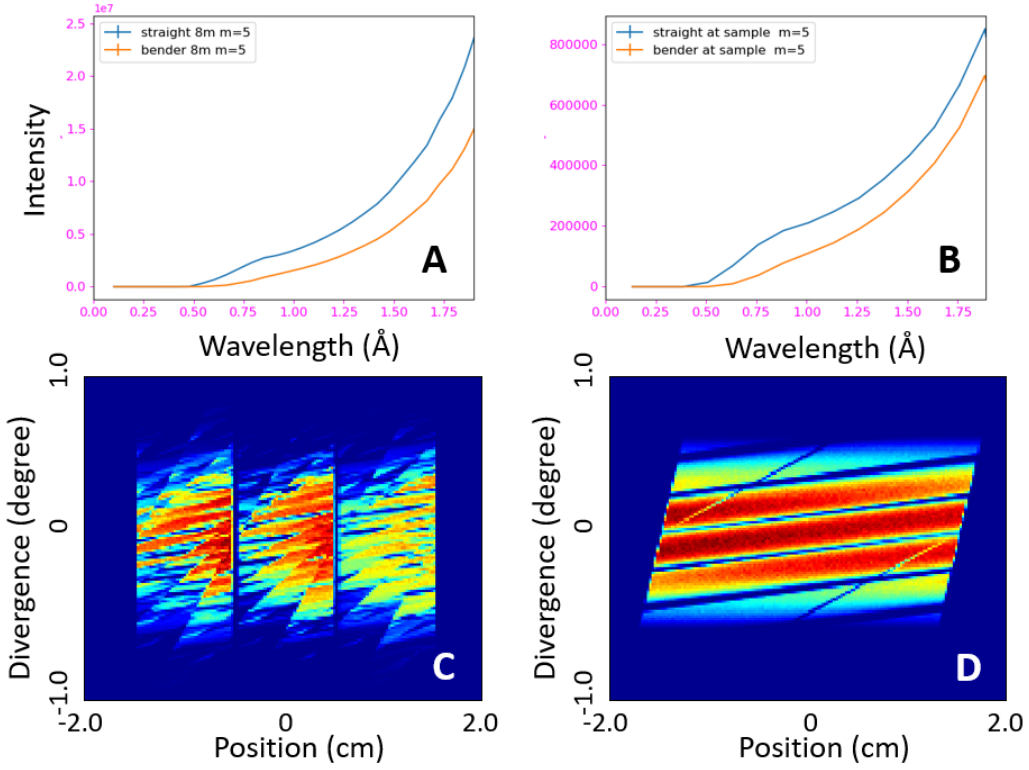

Figure 2. The wavelength band 0.5–2 Å from a bender guide compared with a straight guide (A) at 8 m from the source location; (B) at the nominal sample position. The horizontal acceptance diagram from the wavelength band 2–9.4 Å at 8 m from the source with (C) the bender (D) the straight guide.

Apparently, a straight guide system is superior to transport the much-needed short wavelength for the required wide-angle and diffraction capability of CENTAUR. Therefore, a straight guide system was chosen for the T0 chopper. T0 choppers have been in operation at SNS and other facilities for similar instruments for an extended period, and the reliability and maintenance over the years have proved to be practical. Provisions such as neutron-absorbing baffles will be made during the instrument engineering design phase to minimize background, such as secondary scatterings from a straight beamline.

2.3 Correlation chopper test at CORRELLI

The inclusion of a correlation chopper in CENTAUR offers a distinctive and advantageous capability to suppress inelastic neutron scattering. In many materials, especially hydrogen-rich soft matter systems

such as polymeric, biological, and hydrocarbon materials, the presence of hydrogen in samples or solvents leads to significant inelastic scattering by thermalizing incident neutrons. Even in the case of a 1 mm thick water sample, a portion of neutrons can be thermalized to energies of 2–20 meV, comparable to room temperature thermal energy [9,10]. The misidentification of neutron wavelength caused by inelastic scattering can contaminate the data from time-of-flight (TOF) instruments. Inelastic scattering produces an incoherent background that is difficult to identify and remove from the data [11,12]. This issue has persistently posed challenges for TOF diffractometers because the incoherent inelastic background can substantially degrade the overall signal-to-noise (SNR) ratio, especially in studies involving hydrogenous materials. The energy discrimination capability of a correlation chopper presents an appealing solution.

A correlation chopper employing a pseudorandom opening sequence in its rotor modulates the incident beam by the cross-correlation method [13]. Despite the flux reduction resulting from the 50% duty factor in the pseudorandom opening sequence, the self-correlation property of the sequence, and the recorded chopper phase for each neutron, a correlation chopper operating asynchronously with the source pulse can effectively assign incident neutron energy correctly via statistical analysis. This process corrects the neutron wavelength misidentification during TOF data reduction and significantly reduces the incoherent background arising from inelastic scattering. Consequently, the overall SNR ratio is enhanced even with the flux reduction.

The chopper's energy resolution is determined by Eq. (3):

$$\Delta E/E = \left(\left(2\frac{\Delta t_{ch}}{t_{ch}}\left(1+\frac{L_{ms}}{L_{sd}}\right)\right)^2 + \left(2\frac{\Delta t_m}{t_{ch}}\left(1+\frac{L_{cs}}{L_{sd}}\right)\right)^2\right)^{\frac{1}{2}} \#(3)$$

where Δt_{ch} is the correlation chopper pulse width for each opening, t_{ch} is the TOF from the moderator to the correlation chopper, Δt_m is the pulse emission full width at half maximum (FWHM) from the moderator (given by an empirical function from the moderator design), L_{ms} is the moderator-to-sample the distance, L_{sd} is the sample-to-detector distance, and L_{cs} is the distance from the correlation chopper to the

sample. Based on the geometry in CENTAUR, L_{ms} is 25.5 m, with four detector arrays at L_{sd} of 1.25 m (the backscattering array), 10 m (low-angle), 3.333 m (mid-angle), 1.111 m (high-angle). The correlation chopper can be placed at the end of the guide system so that L_{cs} is 2.76 m. An STS standard medium high-speed chopper has a radius of 0.35 m and operates at 300 Hz. Therefore, a moderate width of 1.5 cm for each pseudorandom opening and neutron energy of 0.2 meV (20 Å) to 200 meV (0.6 Å) provides an energy resolution ($\Delta E/E$) of ~0.4% to 4% at the 10 m detector, ~0.7% to 10% at the 3.33 m detector, ~1.4% to 25% at the 1.111 m detector, and ~1.3 to 25 % at the 1.25 m backscattering detector (Fig. 3). For the lower-energy neutrons that are crucial for SANS and wide-angle neutron scattering (WANS) (e.g., below 20 meV [wavelength >2 Å]), the energy resolution is always better than 8%, which effectively reduces the inelastic event around the thermal energy range, especially for samples using water as a solvent.

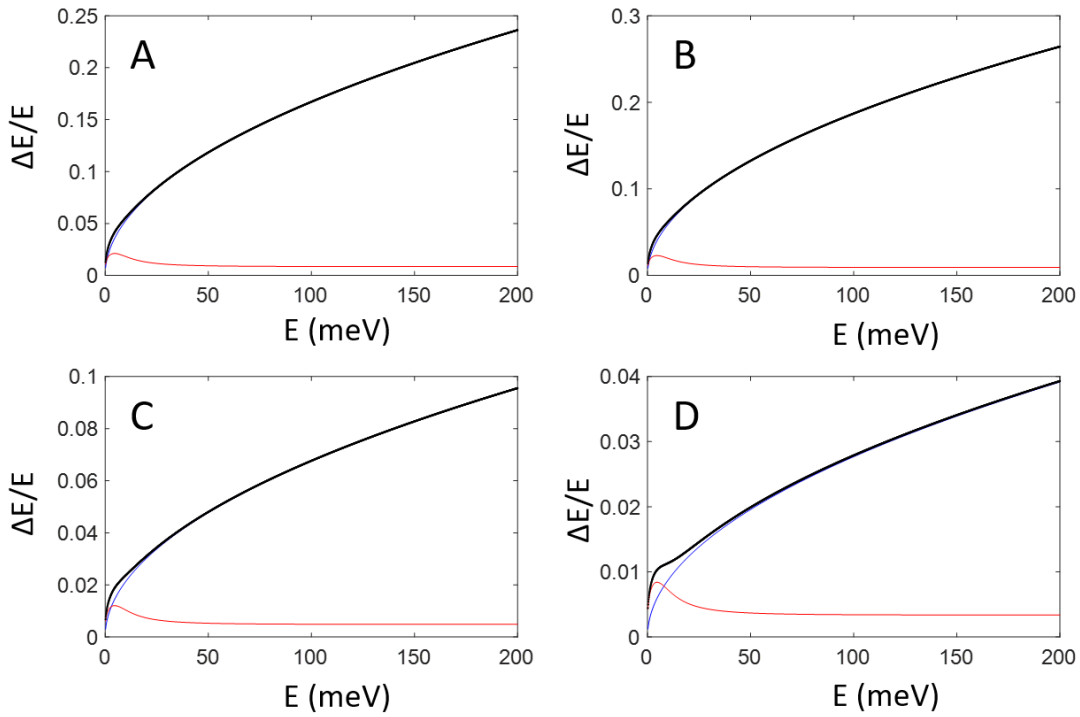

Figure 3. The energy resolution for difference detector arrays: (A) backscattering detector 1.25 m upstream to the sample position; (B) 1.11 m; (C) 3.33 m; (D) 10.0 (m) The red curves are contributions from the moderator (the second term in Eq. [2]), the blue curves are contributions from the correlation chopper, and the black is both contributions combined.

A test experiment was conducted in the CORELLI instrument at SNS because it is the only instrument equipped with a correlation chopper. The goal of this test was to evaluate the chopper's ability to enhance SNR for samples with varying amounts of hydrogen. To emulate these samples, the test used different H_2O/D_2O ratios (100%, 50%, and 0% D_2O and dry powder) of a powder diffraction standard sample (polycrystalline Si from NIST SRM640), which produced little inelastic and incoherent background.

The correlation chopper installed in CORELLI shares similar specifications with the one planned for CENTAUR, featuring a radius of 0.35 m and an operation frequency up to 300 Hz (the SNS First Target Station operates at 60 Hz) at a chopper-to-sample distance of 2 m [13]. As a diffraction instrument, CORELLI's incident energy range covers 10–200 meV, and its sample-to-detector distance (L_{sd}) is 2.5 m. The data acquired were reduced with and without the correlation analysis for comparison, as detailed in the "Methods and Materials" section.

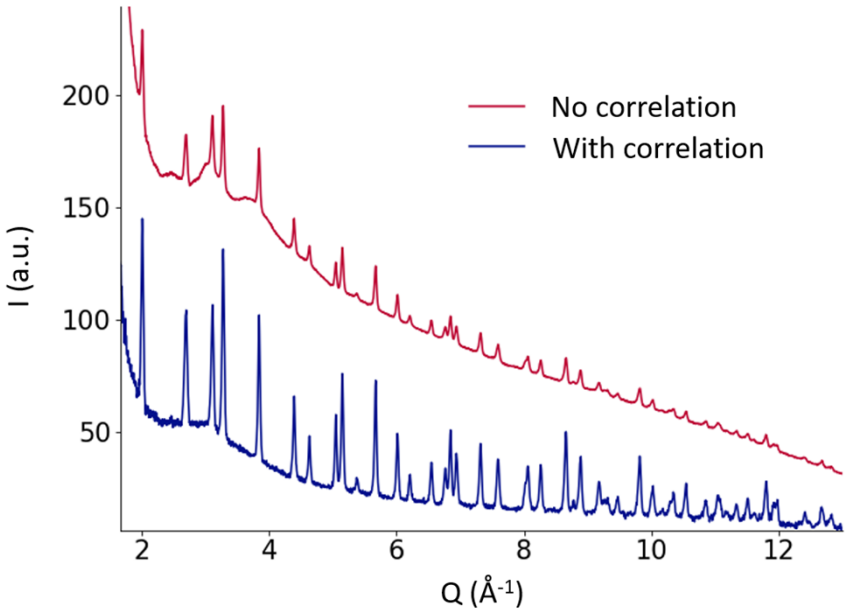

Figure 4. The data from the Si powder diffraction in 100% H_2O (additional peaks from the aluminum sample can are included). The data with the correlation reduction (blue) are of much lower background than those without correlation reduction (red). Other samples are shown in Fig. S3

As shown in Fig. 4 and Fig. S3, correlation chopper significantly reduced the background for all samples. Using the difference between a peak from Si powder and its baseline (the peak prominence) as an indicator for SNR, the SNR enhancement factor (E_f) is given by Eq. (4):

$$E_f = \frac{\left(\mathrm{I_{peak}} - \mathrm{I_{base}}\right)_{\mathrm{corr}}}{\left(\mathrm{I_{peak}} - \mathrm{I_{base}}\right)_{\mathrm{no-corr}}} \#(4)$$

Over the Q range of ~2–13 Å^{-1}, noticeable improvements in SNR were observed with the correlation chopper for all Si peaks (Fig. S4 in SI), despite the reduced total flux. In the most hydrogen-rich sample (100% H_2O), E_f ranges from ~1.4 to 2.8. In the Si 100% D_2O sample, the effectiveness increases as E_f increase from ~1.5 to 7. In less hydrogen-rich samples such as dry Si powder, the improvement is even more significant, up to more than a factor of 20 in E_f, owing to much less incoherent and inelastic scattering from the sample. These results indicate that, in hydrogen-rich samples (e.g., 100%, 50% H_2O), the presence of a substantial amount of incoherent background resulting from inelastic scattering, coupled with multiple scattering in thick samples (such as the aluminum can used in this experiment), tends to overshadow the signals. However, even at the worst case with 100% H_2O, a correlation chopper can improve SNR by ~40%. The improvement is similar to the results from the CANDOR instrument with an energy-analyzed detector[14]. A correlation chopper not only will reduce misidentification of wavelength in inelastic events during data reduction but also will significantly suppress the inelastic incoherent background. Therefore, equipping CENTAUR with a correlation chopper becomes imperative to improve SNR.

CENTAUR will employ a similar specification for the correlation chopper. However, the energy range covered by CENTAUR extends to much colder neutrons, as low as 0.3 meV (16.5 Å). Furthermore, the energy resolution will vary across different detector arrays, as depicted in Fig. 3. Specifically, the 10 m detector will exhibit superb energy resolution, whereas the closer detectors at 1 m will have lower energy resolution. Considering the typical wavelength range employed at CENTAUR (e.g., 1 to 16.5 Å [0.3 to 100 meV]), the energy resolution across all detectors is reasonably good.

3. Neutron optics system optimization

This optimization focused on specifications such as shape, size, m-value, the starting point, and misalignment effect for the non-polarized part of the neutron optics. As shown in Fig. 1, the neutron optics system brings neutrons defined by the bandwidth choppers and provides variable collimation length (hence different divergence) to the sample position around 25.5 m. It can be divided into two parts: (1) the fixed neutron guide and (2) the variable optics system for different collimations. The variable optics system starts at 11 m before the nominal sample position, coinciding with the outer bunker wall. It includes a set of interchangeable components, such as neutron guides, polarization cavity, open space, and source-defining apertures (Figure 1). The first meter is interchangeable between a regular guide and a polarization cavity. The rest provides up to L_1 = 10 m pin-hole collimation distance to the nominal sample position, with three sections of neutron guide in length of 3, 3, and 1 m. Respectively, they provide source-to-sample distances (L_1) of 10, 7, 4, and 3 m (designated as Number of Guide [NG] = 0, 1, 2, 3, respectively). The source-defining apertures can be inserted at the end of the neutron guide as needed. These apertures will be 30 mm in diameter to match the sizes of the neutron guides. Additional components such as smaller apertures may be provided with additional motorized translation stages. At the end of the variable optics system, an evacuated flight tube will extend the beam to the nominal sample position. All components are in vacuum to reduce air scattering and instrument background.

The divergences from collimation distances at CENTAUR (Table 1) are usually better than a typical diffraction instrument. Therefore, no further divergence optimization was pursed for the diffraction functionality. Especially for the backscattering detector, which covers up to 25 $Å^{-1}$ with the short wavelength band, the Q resolution is excellent (SI, Fig. S5). For the forwarding detector arrays, their Q resolutions are dominated by the instrument geometry and are quite good because of the sharp pulse and the instrument's TOF nature. Collimation distances at CENTAUR provide different instrument Q resolutions at different detector arrays. The resolution-smeared data will likely be difficult to merge

without discarding a few points in some cases. Consequently, data sets from the detectors should not be merged and can be fitted at the same time with the same model function.

CENTAUR's design focused on a straight and uniformly sized guide. Although focusing optics, such as elliptical guides, can offer a smaller beam footprint and higher flux intensity at the sample position, the associated increase in divergence may not be suitable for many SANS experiments. Future, more mission-specific SANS instruments at STS, such as those dedicated to biomacromolecule solution scattering, will likely employ advanced focusing optics.

The optimization process assumed a typical sample size of radius 5 mm. However, it does not exclude the use of smaller samples with smaller aperture, although this configuration would result in decreased total intensity on sample. Because the nominal sample position is only 25.5 m away from the neutron source and the maximum collimation distance extends up to 10 m, the influence of gravitational effect between different options is mostly identical. The simulation also showed that even for neutrons with wavelengths longer than 9.5 Å, the gravitational effect has negligible impact on the vertical divergence. Therefore, gravitational effects will be ignored for the purposes of this discussion.

3.1 The shape of the guide: square vs. octagon

Typically, neutron guides on beamlines are rectangular or square. However, considering the tube-shaped moderator with a diameter of 3 cm and a round sample aperture, a neutron guide that resembles such a shape may utilize the source brightness more effectively. Consequently, the performances of square and octagonal guide systems were compared. An octagonal guide system is a practical solution to match the moderator shape and is readily available from various manufacturers. The results clearly demonstrate the superiority of the octagonal guide over the square guide.

A comparison of a 3 × 3 cm square guide with an octagonal guide with the same dimensions between two parallel sides, effectively matching the source size as depicted in Fig. 5A and B, reveals that the brilliance transfer of the octagonal guide is significantly better across various neutron guides (Fig. 6).

The integrated flux over a typical wavelength ranging from 2 to 9.44 Å increases by approximately 15%, particularly for longer wavelength neutrons (>2.5 Å), which are highly desirable for CENTAUR. Although the maximum divergence remains unchanged, the phase space is significantly better filled with the octagonal guide owing to reduced under-illumination by the source. Consequently, the divergence uniformity improves considerably, as evidenced by Fig. 5C and 5D. Notably, the unfilled strip observed in NG = 3 (Fig. 5E) is now filled (Fig. 5F), thanks to the more gradual transition between the reflecting supermirror surfaces in the octagonal geometry. Although small-angle scattering in general is forgiven for a phase space gap or pattern, sharper features in certain samples as well as diffraction data will benefit from the improved phase space provided by the octagonal guide.

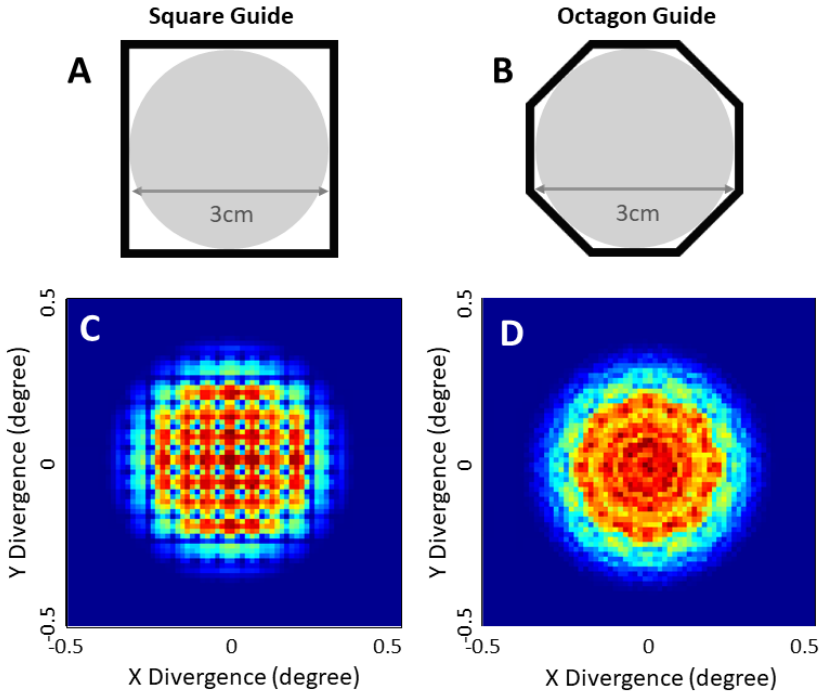

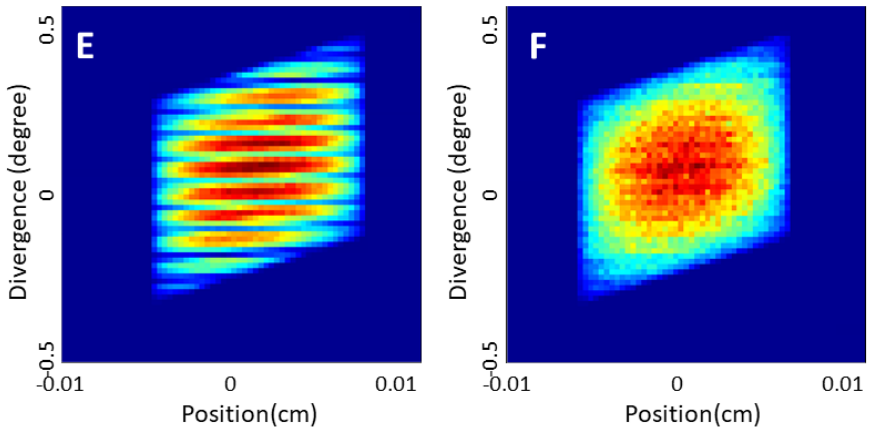

Figure 5. The shape of (A) the square guide and (B) the octagonal guide with dimensions labeled. The shaded circles inside represent the tube moderator size and dimension for comparison. The divergence profiles are at the sample position with NG = 3 for (C) the square guide and (D) the octagonal guide. The acceptance diagrams are at the sample position with NG = 3 for (E) the square guide and (F) the octagonal guide.

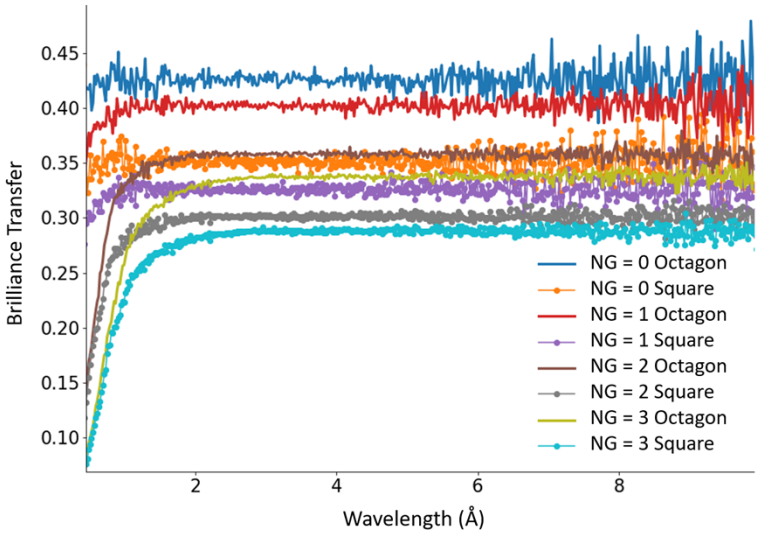

Figure 6. Brilliance transfer from the octagonal guide system (line) compared with the square guide system (dot-line) at NG = 0, 1, 2, 3 with guide coating m = 3.

3.2 Starting location, size and supermirror m-value.

The optimization of the octagonal guide was extended to include the starting location, m-value, and size.

Depending on the location of the beam port, the guide's starting position can be as close as approximately

0.8 m from the moderator face. To ensure the guide's longevity in the high-radiation and high-temperature environment, metallic substrates such as copper will be utilized. Moving the guide's starting point farther away (e.g., 1.3, 1.8, or 2.3 m from the moderator) may also help. The performance and optimization of different starting points were investigated accordingly. The selection of the m-value for the supermirror coating is crucial for efficient neutron transport and cost control. The optimization and performance changes were examined under various collimation scenarios at NG = 0, 1, 2, and 3.

In general, the brilliance transfer for neutron wavelengths greater than 2 Å remains the same across different m-values (Fig. 7). However, for shorter wavelengths ranging from 0.5 to 2 Å, which are vital for wide-angle scattering and diffraction capabilities, higher m-values consistently outperform lower ones. This result is illustrated for the case of NG = 3 in Fig. 7. Considering the significance of the 0.5–2 Å wavelength range, an m-value of 3 was determined to be a cost-effective choice. It is nearly identical to higher m-values for wavelengths above 1 Å and significantly superior to lower m-values for wavelengths between 0.5 and 1 Å.

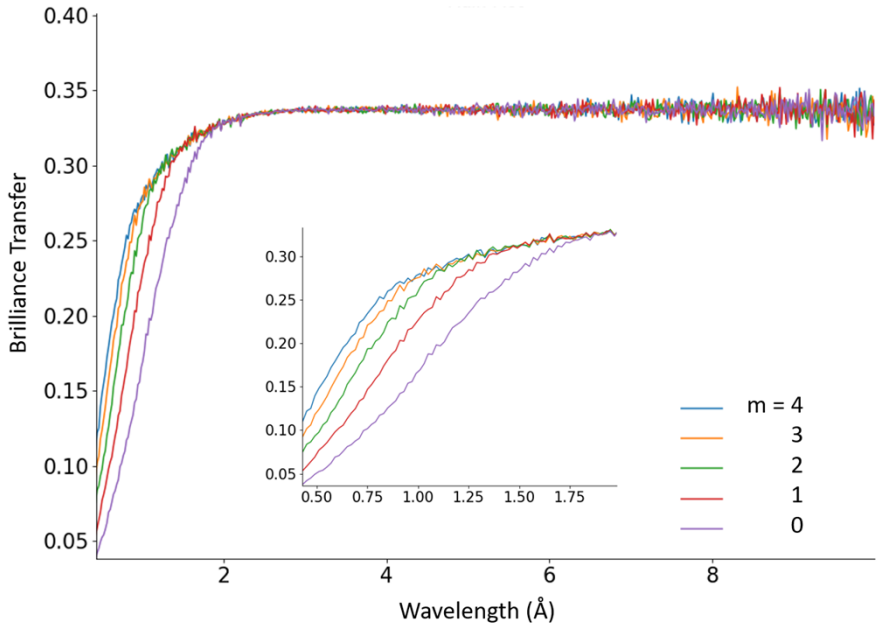

Figure 7. Brilliance transfer for different m-values at NG = 3. The inset shows a detail view of the shorter wavelength from 0.5 to 2 Å.

For the longest collimation distance of 10 m (NG = 0), moving the starting point away from the source in 0.5 m increments results in a negligible 1% reduction in flux, as expected. However, for other collimation distances, the flux decreases by approximately 4% for every 0.5 m displacement. Therefore, the core guide's starting point should be positioned as close to the moderator as practically feasible.

The relationship between the size of the octagonal guide, different values of NG, and the starting point of the guide is intricate owing to the interplay of moderator, guide, and collimation distance [15]. Tests were conducted using octagonal guides sizes ranging from 3.1 to 2.6 cm. The octagon's size is defined as in Fig. 5B: an octagon larger than the moderator results in under-illumination, and an octagon smaller than the moderator results in over-illumination. In most cases, a 3 cm guide provided superior integrated flux throughout the required bandwidth. Occasionally, shorter collimation distances (e.g., NG = 2 or 3) and smaller guide sizes (2.8 or 2.9 cm) result in a slight increase in brilliance transfer because of smaller divergences, but the integrated flux remained lower than with the 3 cm guide. Similar results were also observed with the square guide system. The slightly increased divergence with a 3 cm guide is inconsequential for SANS, WANS, and diffraction. A guide that is larger than the source diameter offers no benefits. Therefore, the optimal size for the octagonal guide is 3 cm.

Unavoidable gaps are present in the guide system to accommodate the choppers and vacuum windows. For instance, the T0 chopper requires a gap of approximately 0.5 m, and the large single-disc chopper requires gaps of 0.07 m in the guides. Test results indicate that a 0.2 m gap can reduce the integrated flux at the sample position by up to 7%, particularly affecting the shorter wavelengths crucial for WANS and diffraction. However, a smaller gap on the order of 5 mm shows only marginal impact.

The resulting divergence and flux from typical instrument configurations are listed in Table 1. The selected divergence and phase diagrams are shown in Fig. S6.

Table 1. CENTAUR *Q* range and flux at sample at selected instrument configurations based on the STS source file *ST-17-TU90D-TINT-March_2022.dat* (2022). The *Q* range was calculated based on detector coverage with the wavelength band λ_{min} to λ_{max} for Q_{max} and Q_{min}, respectively.

Configuration	Wavelength range (Å)	*Q* range (Å^{-1}) (forwarding detectors)	*Q* range (Å^{-1}) (backscattering detector)	Divergence FWHM at the sample	Flux at sample (n s^{-1} cm^{-2})
15 Hz, NG = 0	2.00–9.44	0.0016–1.9	1.4–6.25	0.142°	8.79×10^7
15 Hz, NG = 1	2.00–9.44	0.0023–1.9	1.4–6.25	0.198°	1.74×10^9
15 Hz, NG = 2	2.00–9.44	0.0039–1.9	1.4–6.25	0.334°	4.81×10^8
15 Hz, NG = 3	2.00–9.44	0.0056–1.9	1.4–6.25	0.404°	7.95×10^8
15 Hz, NG = 3	1.00–8.44	0.0063–3.8	1.25–13.50	0.404°	8.71×10^8
7.5 Hz, NG = 0	0.50–15.36	0.001–5.86	0.83–25.0	0.142°	5.08×10^7
7.5Hz, NG = 3	0.50–15.36	0.0035–5.86	0.83–25.0	0.404°	4.56×10^8

3.3 Rapid mode switching

Performing experiments with fast kinetics may require measuring the sample in different modes, such as high-flux (a more diverged beam but better for diffraction) and high-resolution (a better collimated beam but better for SANS) modes. Traditionally, the method of changing the beam characteristics on the sample involved moving neutron guides in and out of the beam path. However, because the guides are so delicate, this process requires slow translational motion. Reducing the mode switch to less than 1 s will make such measurement practical. Simultaneously, the detectors at a SANS instrument must be repositioned for needed *Q* coverage.

To address the challenge of rapid mode switching, a series of rapid variable apertures were developed and placed between the guide sections at 7, 4, and 3 m from the sample position (Fig. 8). Instead of moving the fragile guides, smaller apertures, as opposed to the typical 15 mm radius of the source defining aperture, can be inserted into the gaps between the variable guide system. Once inserted, they effectively reduce the effectiveness of the guides and further collimate the beam without the need to move the guides. Given that the detectors at CENTAUR are already fixed in position with a generous solid-angle coverage, this technique is ready for implementation.

During the simulation, using these rapid variable apertures in the high-flux mode (NG = 3) resulted in comparable Q_{min} values and flux as those obtained in the high-resolution mode (NG = 0). For example, with aperture sizes 12, 7, and 5 mm, the divergence FWHM at the sample was 0.15° degrees and flux was 8.29×10^7 n s^{-1} cm^{-2} (Fig. S7), which is close to the longest collimation achieved in NG = 0 (Table 1, 15 Hz, NG=0).

To minimize the gap between the variable guides, the thickness of such apertures will be less than 5 mm. Moreover, by incorporating apertures with different radii or an iris-style variable aperture (currently under development at STS), further flexibility in divergence and beam profile can be achieved. If the thin iris-style aperture is successfully developed, then the guides in the system will be fixed, eliminating any need for large-guide translational motion.

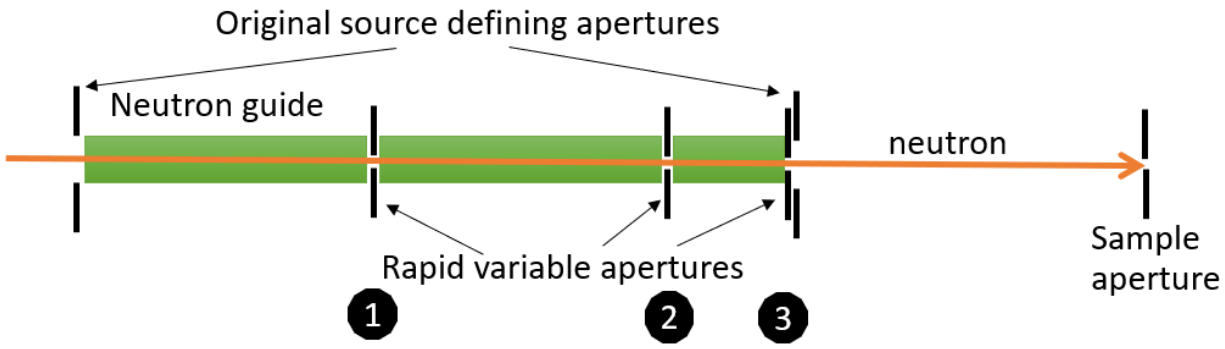

Figure 8. Aperture setup diagram for the rapid mode switching. The rapid variable aperture 1, 2, 3 are located 7, 4, and 3 m, respectively, upstream of the sample position.

3.4 Guide misalignment test

The neutron guides utilized in the system consist of shorter pieces, typically 0.5 m long, which are assembled into longer sections as required. During the assembly and installation process, careful consideration must be given to small misalignments to ensure the desired performance. This study examined the effect of misalignment on brilliance transfer. Generally, misalignment issues take one of two forms: (1) systematic misalignment caused by vertical ground deformation on the floor of the conventional facility building and (2) random misalignment of the optical components within the

instrument. For the systematic misalignment, the floor is expected to settle within a few months after the installation of the heaviest component, the target monolith. Therefore, at the time of CENTAUR installation, the floor is assumed to be stable and fully settled. The study by Lin et al. showed that the systematic misalignment with a small vertical settlement will not significantly affect instrument performance [16]. Therefore, the primary focus of the present misalignment study is the random misalignment, which refers to deviations from the specified ideal locations of optical components introduced during manufacturing and installation processes.

First, the study found the longitudinal displacement along the neutron beam direction showed little impact on the performance, even up to the millimeter range, because of the typical long collimation length in a SANS instrument. The results showed another benefit of the octagonal guide: it is more rotationally forgiving because the shape is more symmetrical than a square. The whole guide system is quite tolerant for misalignment. For example, the most stringent configuration for alignment is that at NG = 3 because all guides are in the beam path. The simulation of this configuration showed that misalignments of section transversal of 50 μm, section rotational of 4 mrad, element transversal of 20 μm, and elemental rotational of 0.8 mrad reduce brilliance transfer by only about 5% over the wavelength band (Figure 9). These alignment accuracies are typically achievable by the SNS survey and alignment team. Even the worst case tested (misalignments of section transversal of 200 μm, section rotational of 8 mrad, element transversal of 100 μm, and element rotational of 2 mrad) reduces the performance by about 30% at NG = 3 with acceptable divergence and phase space (Fig. S8). This result indicates that the optical system is robust and will perform well under the foreseeable circumstances.

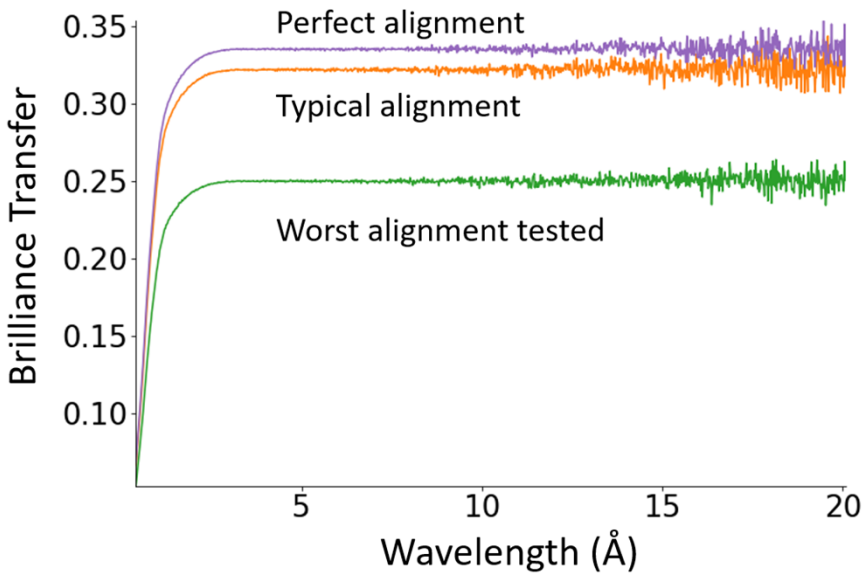

Figure 9. Brilliance transfer at different alignment scenarios tested.

Conclusion

CENTAUR's specifications are guided by its scientific mission to cater to a broad user community spanning diverse research areas, from soft matter to hard matter and fundamental basic research to applied materials research. This work involved optimizing the chopper system and the neutron guide system for CENTAUR. The result is a versatile SANS instrument with much needed WANS and diffraction capability. The use of octagonal guides, a correlation chopper, and other parameters explored in this study will significantly improve CENTAUR's performance.

Acknowledgement

This research used resources of the SNS STS Project at ORNL. A portion of this research used resources at SNS, a US Department of Energy (DOE) Office of Science user facility operated by ORNL. ORNL is managed by UT-Battelle LLC for DOE's Office of Science. We thank Drs. John Anker, Yaohua Liu, Gabriele Sala, Leighton Coates and Kenneth Herwig for helpful discussions and for assisting with various calculations.

References

[1] S.(钱朔) Qian, W. Heller, W.-R. Chen, A. Christianson, C. Do, Y. Wang, J.Y.Y. Lin, T. Huegle, C. Jiang, C. Boone, C. Hart, V. Graves, CENTAUR—The small- and wide-angle neutron scattering diffractometer/spectrometer for the Second Target Station of the Spallation Neutron Source, Rev. Sci. Instrum., 93 (2022) 075104.

[2] Oak Ridge National Laboratory, SPALLATION NEUTRON SOURCE SECOND TARGET STATION CONCEPTUAL DESIGN REPORT VOLUME 1: OVERVIEW, TECHNICAL AND EXPERIMENT SYSTEMS, (2020).

[3] L. Zavorka, K. Ghoos, J. Risner, I. Remec, An unstructured mesh based neutronics optimization workflow, Nucl. Instrum. Methods Phys. Res. Sect. Accel. Spectrometers Detect. Assoc. Equip., 1052 (2023) 168252.

[4] K.H. Andersen, M. Bertelsen, L. Zanini, E.B. Klinkby, T. Schönfeldt, P.M. Bentley, J. Saroun, Optimization of moderators and beam extraction at the ESS, J. Appl. Crystallogr., 51 (2018) 264–281.

[5] J.M. Carpenter, D.F.R. Mildner, Neutron guide tube gain for a remote finite source, Nucl. Instrum. Methods Phys. Res., 196 (1982) 341–348.

[6] J.R.D. Copley, The joy of acceptance diagrams, J. Neutron Res., 1 (1993) 21–36.

[7] Y. Liu, H. Cao, S. Rosenkranz, M. Frost, T. Huegle, J.Y.Y. Lin, P. Torres, A. Stoica, B.C. Chakoumakos, PIONEER, a high-resolution single-crystal polarized neutron diffractometer, Rev. Sci. Instrum., 93 (2022) 073901.

[8] S. Qian, C. Jiang, F. Li, A. Khaplanov, Conceptual Polarization Setup at CENTAUR, the SANS/WANS Instrument at the Second Target Station of SNS, in: J. Phys. Conf. Ser., IOP Publishing, 2023: p. 012002.

[9] C. Do, W.T. Heller, C. Stanley, F.X. Gallmeier, M. Doucet, G.S. Smith, Understanding inelastically scattered neutrons from water on a time-of-flight small-angle neutron scattering (SANS) instrument, Nucl. Instrum. Methods Phys. Res. Sect. Accel. Spectrometers Detect. Assoc. Equip., 737 (2014) 42–46.

[10] A.R. Rennie, R.K. Heenan, International seminar on structural investigations on pulsed neutron sources Proceedings, in: JINR, Russian Federation, 1993.

[11] J.G. Barker, D.F.R. Mildner, Survey of background scattering from materials found in small-angle neutron scattering, J. Appl. Crystallogr., 48 (2015) 1055–1071.

[12] L. Balacescu, G. Brandl, A. Radulescu, Separation of the inelastic and elastic scattering in time-of-flight mode on the pinhole small-angle neutron scattering diffractometer K-WS-2, J. Appl. Crystallogr., 54 (2021) 1217–1224.

[13] F. Ye, Y. Liu, R. Whitfield, R. Osborn, S. Rosenkranz, Implementation of cross correlation for energy discrimination on the time-of-flight spectrometer CORELLI, J. Appl. Crystallogr., 51 (2018) 315–322.

[14] D.P. Hoogerheide, J.A. Dura, B.B. Maranville, C.F. Majkrzak, Low-background neutron reflectometry from solid/liquid interfaces, J. Appl. Crystallogr., 55 (2022) 58–66.

[15] J.K. Zhao, J.L. Robertson, K.W. Herwig, F.X. Gallmeier, B.W. Riemer, Optimizing moderator dimensions for neutron scattering at the spallation neutron source, Rev. Sci. Instrum., 84 (2013) 125104.

[16] J.Y.Y. Lin, T. Huegle, L. Coates, A.D. Stoica, A realistic guide misalignment model for the Second Target Station instruments at the Spallation Neutron Source, Nucl. Instrum. Methods Phys. Res. Sect. Accel. Spectrometers Detect. Assoc. Equip., 1047 (2023) 167881.